Atmos. Chem. Phys. Discuss., 12, 5705–5738, 2012
www.atmos-chem-phys-discuss.net/12/5705/2012/
doi:10.5194/acpd-12-5705-2012

Atmospheric Chemistry and Physics Discussions

Methanol-CO correlations in Mexico City pollution outflow from aircraft and satellite during MILAGRO

Y. Xiao[1], K. E. Cady-Pereira[1], V. H. Payne[1], D. B. Millet[2], M. W. Shephard[3], M. Luo[4], M. Alvarado[1], K. C. Wells[2], E. C. Apel[5], T. L. Campos[5], H. B. Singh[6], and G. W. Sachse[7]

[1]Atmospheric and Environmental Research, Inc., Lexington, Massachusetts, USA
[2]University of Minnesota, Department of Soil, Water and Climate, St. Paul, Minnesota, USA
[3]Atmospheric and Climate Applications (AC Apps), Inc., East Gwillimbury, Ontario, Canada
[4]Jet Propulsion Laboratory, California Institute of Technology, Pasadena, California, USA
[5]National Center for Atmospheric Research, Boulder, CO, USA
[6]NASA Ames Research Center, CA, USA
[7]NASA Langley Research Center, VA, USA

Received: 19 December 2011 – Accepted: 18 January 2012 – Published: 22 February 2012

Correspondence to: Y. Xiao (yxiao@aer.com)

Published by Copernicus Publications on behalf of the European Geosciences Union.

Abstract

The correlation between methanol (CH_3OH) and carbon monoxide (CO) is of particular interest for characterizing biogenic and anthropogenic emission sources of CH_3OH and other chemical species. Here, the CH_3OH/CO enhancement ratio ($\Delta CH_3OH/\Delta CO$) in the lower to middle troposphere is examined using coincident CH_3OH and CO observations from aircraft (NCAR C-130 and NASA DC-8) and from the Tropospheric Emission Spectrometer (TES) satellite during the MegaCity Initiative: Local and Global Research Observations (MILAGRO) in the Mexico City region in March 2006. $\Delta CH_3OH/\Delta CO$ ratios from the two in-situ aircraft measurements are far higher than previously reported CH_3OH emission ratios relative to CO from US cities. This may reflect combustion of different fuel types in this area, and possibly photochemical production of CH_3OH in Mexico City outflow. TES CH_3OH and CO retrievals over the MILAGRO domain show relatively high sensitivity in the 600–800 hPa range, associated with Mexico City pollution outflow. The TES derived $\Delta CH_3OH/\Delta CO$ ratios during MILAGRO are 18–24 ppt ppb^{-1}, which are similar to those observed from the DC-8 (26–39 ppt ppb^{-1}), but lower than the C-130 observations (41–55 ppt ppb^{-1}). Differences between the $\Delta CH_3OH/\Delta CO$ ratios measured aboard the two aircraft preclude an absolute validation of the TES-derived ratios for this dataset. The $\Delta CH_3OH/\Delta CO$ ratios observed from TES over this domain reflect bulk enhancements of CH_3OH and CO in Mexico City outflow. Although the TES measurements are not expected to resolve small-scale variability in the $\Delta CH_3OH/\Delta CO$ ratio downwind of the strong source region of Mexico City, it is demonstrated that TES can clearly distinguish differences in the $\Delta CH_3OH/\Delta CO$ ratio due to different source categories of CH_3OH. An example of this is shown by contrasting measurements over Mexico City (strong anthropogenic emissions) with those over the Amazon Basin (strong biogenic emissions). The results from this case study show the potential to gain insight into global sources of CH_3OH and related species from satellite observations, especially for regions and time periods where no in situ measurements are available.

ACPD

12, 5705–5738, 2012

1 Introduction

Methanol (CH_3OH) is one of the most abundant volatile organic compounds (VOCs). It is a significant source of tropospheric carbon monoxide (CO) and formaldehyde (CH_2O) (Duncan et al., 2007; Millet et al., 2005; Hu et al., 2011). CH_3OH can also have an important influence on air quality in and around polluted urban areas (Molina et al., 2010). CH_3OH may also contribute to particulate pollution (Blando and Turpin, 2000). The first global detection of methanol was made by Singh et al. (1995). Globally the major sources of CH_3OH are biogenic processes with ~50 %–80 % of the estimated emissions involving plant growth (Harley et al., 2007; Karl et al., 2003) and, to a lesser extent, plant decay (Warneke et al., 1999). Other sources include biomass burning (Paton-Walsh et al., 2008; Dufour et al., 2006), anthropogenic sources from vehicles and industrial activities (de Gouw et al., 2005, 2009), as well as oxidation of methane and other volatile organic compounds (Tyndall et al., 2001; Madronich and Calvert, 1990). Although these other sources are much less important than the biogenic source on a global scale, they can be responsible for large CH_3OH enhancements on regional or continental scales. The main sink of CH_3OH is oxidation by OH (Heikes et al., 2002). Dry and wet deposition to the surface constitutes a minor sink (Karl et al., 2010). The resulting overall atmospheric lifetime of CH_3OH is approximately 5–10 days (Jacob et al., 2005).

Estimates of the source strength, seasonality, and spatial distribution of CH_3OH in the atmosphere have previously been obtained from field measurements (e.g. Heikes et al., 2002; Singh et al., 2000), chemical transport modeling in combination with ground and airborne measurements of CH_3OH (e.g. Millet et al., 2008; Jacob et al., 2005; Tie et al., 2003; Galbally and Kirstine, 2002), and from remotely sensed measurements from ground-based infrared spectrometers (e.g. Rinsland et al., 2009; Paton-Walsh et al., 2008). These studies have provided much-needed insight into CH_3OH sources and atmospheric abundance. However, large uncertainties persist in terms of CH_3OH source magnitudes, seasonality, and its spatial distribution in the atmosphere.

ACPD
12, 5705–5738, 2012

Satellite measurements offer the advantage of high spatial and temporal coverage, albeit with lower resolution than in situ observations. For example, CH_3OH has been measured in biomass burning plumes in the upper troposphere from the Atmospheric Chemistry Experiment Fourier Transform Spectrometer (ACE-FTS), a limb-viewing instrument with relatively high vertical resolution and sensitivity to minor trace gases (Coheur et al., 2007; Dufour et al., 2006). More recently, it has been shown that nadir instruments can measure enhanced CH_3OH in the lower troposphere. CH_3OH retrievals have been performed using data from the Tropospheric Emission Spectrometer (TES) on the NASA Aura satellite (Cady-Pereira et al., 2012; Beer et al., 2008) and from the Infrared Atmospheric Sounding Instrument (IASI) onboard the polar-orbiting MetOp-A satellite (Razavi et al., 2011). In addition, TES and IASI observations have been employed to better constrain the seasonality of methanol emissions from northern mid-latitude ecosystems (Wells et al., 2012) and to constrain biogenic and biomass burning emissions of methanol (Stavrakou et al., 2011). Both TES and IASI use the same spectral region (centered at $1033\,cm^{-1}$) for CH_3OH retrieval. TES has high spectral resolution of $0.06\,cm^{-1}$ at nadir providing the ability to distinguish the target species from interferences, while the IASI instrument has larger spatial coverage providing global coverage twice per day due to the wide scans across its track.

Constraints on the importance of various CH_3OH source types can be gained by examining the correlations between CH_3OH and other measured species. The correlation between CH_3OH and CO is of particular interest in source characterization (Warneke et al., 2007; de Gouw et al., 2005), and simultaneous measurements of CH_3OH and CO are available from the satellite instruments listed above. CH_3OH and CO share common anthropogenic and biomass burning sources. However, biogenic CH_3OH emissions can modify the CH_3OH-CO ratio to varying degrees depending on their importance relative to combustion sources. In general, both molecules exhibit a similar vertical distribution since their sources are mainly at the surface, although both CH_3OH and CO do have atmospheric sources from the oxidation of CH_4 and other volatile organic compounds (Madronich and Calvert, 1990).

ACPD
12, 5705–5738, 2012

The Megacity Initiative: Local And Global Research Observations (MILAGRO) field campaign was conducted over the Mexico City Metropolitan Area (MCMA) and the Gulf of Mexico in March 2006, with the goal of examining the properties, evolution, and export of atmospheric emissions of trace gases and particles generated in the MCMA and to evaluate the regional and global impacts of these emissions (Molina et al., 2010; Singh et al., 2009). Major sources of pollutants in the MCMA include motor vehicles (Apel et al., 2010), pervasive incomplete combustion of fossil fuels including Liquid Petroleum Gas (LPG) for low-temperature household cooking and heating (Blake and Rowland, 1995), and biomass burning (Crounse et al., 2009; Yokelson et al., 2007). During MILAGRO, urban and regional measurements of a number of air pollutants were obtained by the National Center for Atmospheric Research (NCAR) C-130 and the National Aeronautics and Space Administration (NASA) DC-8 aircraft. In this analysis, we utilize MILAGRO aircraft measurements to determine correlations between CH_3OH and CO, as well as between CH_3OH and other trace gas pollutants, in order to qualitatively assess the influence of different sources on the CH_3OH concentrations in the Mexico City outflow.

During MILAGRO TES also made a number of special observations over the MCMA. Retrievals of CH_3OH and CO have been performed based on these observations. Direct comparisons of aircraft in situ profiles of CH_3OH and CO with satellite retrievals during MILAGRO proved challenging as there were very few targeted profile underflights of the satellite track by either the C-130 or DC-8 aircraft over Mexico City, which limited sampling coincidence within reasonable spatial and temporal criteria. Instead, we have utilized CH_3OH-CO correlations to evaluate the ability of the satellite data to capture the important source information offered by aircraft measurements, with the goal of assessing whether such space-borne data can be reliably applied to other regions and time periods where no aircraft measurements are available. In addition, in order to further explore the utility of CH_3OH-CO correlations from TES, we have compared and contrasted satellite CH_3OH-CO correlations from MILAGRO (dominated by anthropogenic emissions – e.g. Molina et al., 2010) with those over the Amazon Basin

ACPD
12, 5705–5738, 2012

(dominated by biogenic emissions – e.g. Karl et al., 2007).

Descriptions of the aircraft and TES satellite measurements are provided in Sect. 2, and the analysis and results in Sect. 3.

2 Measurements during MILAGRO

2.1 Aircraft measurements

Figure 1 shows the aircraft flight tracks (along with TES footprint locations) during MILAGRO. All the data used in this work were collected within 12° N–30° N and 102° W–90° W, covering the region downwind of Mexico City and the northern part of the Gulf of Mexico. The MCMA (19.43° N, 99.12° W) is located in the Valley of Mexico, a large basin 2.2 km a.s.l. The basin is surrounded on three sides by mountain ridges, with a broad opening to the north. The C-130 flight tracks are closer than those of the DC-8 to the urban area of Mexico City, though some of the flights were designed to fly over remote regions either to detect long-range plume transport (more than 1000 km from Mexico City) or to measure biomass burning plumes. The DC-8 flight tracks cover a larger geographical domain and the measurements are more representative of outflow at a distance from the sources.

Airborne measurements of CH_3OH were made by the Total Organic Gas Analyzer (TOGA) (Apel et al., 2010) onboard the C-130, and the Peroxy Acetyl Nitrate/Aldehyde/Ketone Photo Ionization Detector (PANAK) (Singh et al., 2004) onboard the DC-8. The reported CH_3OH uncertainty for both aircraft instruments is 20 % at 1σ level. However, intercomparisons of TOGA (C-130) and PANAK (DC-8) measurements during MILAGRO have shown that the CH_3OH values from the C-130 are generally higher than those from the DC-8, by as much as a factor of 2. This suggests a possible inconsistency in calibration between the CH_3OH measurements onboard the two aircraft (Kleb et al., 2011, more details at http://www-air.larc.nasa.gov/missions/intex-b/intexb-meas-comparison.htm).

ACPD
12, 5705–5738, 2012

Volume mixing ratios of CO were measured by the Ultra-Violet Fluorescence (UVF) instrument on the C-130 (Holloway et al., 2000) with a quoted accuracy of 10 %, and by the Differential Absorption CO Measurement (DACOM) instrument (Sachse et al., 1987), a mid-IR diode laser spectrometer that measured CO, CH_4, and N_2O on the DC-8 aircraft. DACOM's quoted CO accuracy is 2 % or 2 ppb. A suite of simultaneous observations of other related hydrocarbons on the C-130 aircraft are also used in Sect. 3 for quantification of the source signature of CH_3OH. All those species were measured with an estimated accuracy of ≤20 % (Singh et al., 2009). The MILAGRO data is supplied on a 1 min merge. However, the TOGA CH_3OH measurements were actually made with 2.8 min temporal resolution. Therefore, in this analysis we have further merged the data to 3 min intervals for instances where CO differs by more than 10 ppb between time steps, but CH_3OH values are constant. To reduce the influence of a small number of extreme outliers on the correlation analysis, we removed any data with CO concentrations greater than 500 ppb. These points were all located within 300 km of the city center and comprised around 3 % of the whole dataset. Any errors in the airborne CH_3OH and CO measurements are assumed independent and not taken into account for the correlation analysis in Sect. 3.

2.2 Satellite measurements from TES

TES is a Fourier transform spectrometer flying on the NASA Aura satellite. The instrument has high spectral resolution (0.06 cm^{-1}) and a relatively small (5 × 8 km) nadir footprint. The TES instrument measures radiances in the spectral range 650 to 3050 cm^{-1} (Beer et al., 2001) that are very stable (Conner et al., 2011) with good radiometric calibration and signal-to-noise (Shephard et al., 2008). These instrument characteristics provide TES with the capability to provide information on the vertical profiles of temperature and numerous trace gases in the atmosphere. Profiles of temperature, water vapor (H_2O and HDO), ozone (O_3), CO, methane (CH_4) and ammonia (NH_3) are currently produced routinely as operational products (Version 5). Other trace gas products, including CH_3OH, are currently under development to be implemented

ACPD
12, 5705–5738, 2012

operationally. CH_3OH is scheduled to be processed routinely as part of the TES Version 6 algorithm release.

TES conducted several special "step-and-stare" observations during the MILAGRO campaign. The TES nadir footprints in these observations are separated by ~45 km along the Aura ground track. The Aura overpass times for Mexico City are 01:45 and 13:45 LT.

The first space-based nadir retrievals of CH_3OH were reported by Beer et al. (2008) for a limited number of TES special observations over Beijing (Northeast China), and San Diego (California, USA). Since then, the TES CH_3OH retrieval approach has been developed further and applied to larger volumes of data. The algorithm is based on an optimal estimation approach with a priori constraints. Details of the retrieval algorithm are reported in Cady-Pereira et al. (2012). The TES retrieval errors for CH_3OH during MILAGRO range from 10 % to 50 %, with larger relative errors for small retrieved CH_3OH values. The TES retrievals have been validated against vertical profiles from an ensemble of aircraft measurements over North America, where a 3-D chemical transport model was used as an intercomparison platform (Wells et al., 2012).

The TES operational CO product (Version 4) used in this analysis has been extensively validated against aircraft and other satellite measurements (Luo et al. 2007a, 2007b; Lopez et al., 2008), and showed a negative bias of <10 % in the lower and middle troposphere near Houston during INTEX-B and a positive bias of ~5–10 % in the tropics. Here we assume no correlation between the TES measurement errors for CH_3OH and CO as they are in retrieved in different spectral bands. Any measurement errors should thus have little impact on the derived CH_3OH-CO enhancement ratios.

Figure 2 shows example averaging kernels for both CH_3OH and CO. Both species have peak sensitivity in the 600–800 hPa region. The TES CO and CH_3OH retrievals contain a limited amount of vertical information, with ~1.4 degrees of freedom for signal (DOFS) for CO and typically <1 for CH_3OH. The vertical resolution for TES CH_3OH and CO retrievals (defined as the full width at half maximum of the averaging kernels) is about 5–6 km in the troposphere.

ACPD
12, 5705–5738, 2012

For both species, the number of vertical levels used in the retrieval is significantly greater than the number of DOFS for the measurement. Performing the retrieval in this way allows variations in vertical sensitivity between different profiles to be characterized via the averaging kernels. However, it also means that the details of the result on any given retrieval level are highly sensitive to the shape of the chosen a priori profile. In order to mitigate this issue, a post-processing step is performed to map the result from the relatively fine retrieval grid to a representation that better reflects the information available in the measurement. The exact details of the mapping depend on the sensitivity (averaging kernels) for each individual measurement. For CH_3OH with ~1 (or less) DOFS, we report a single "representative volume mixing ratio" (RVMR) value. Further details of this approach can be found in Payne et al. (2009) and Shephard et al. (2011). The end result is that the RVMR value is less sensitive to assumptions about the a priori profile shape than a value at a single retrieval level would be. In order to assess the CH_3OH-CO correlations, the CH_3OH-sensitivity-based mapping was also applied to the CO retrieval in each case to produce a "pseudo CO RVMR". The same approach has been used to determine the emission ratio of ammonia and formic acid relative to CO using TES observations of boreal biomass plumes (Alvarado et al., 2011). In addition, an acceptance criterion of the CH_3OH RVMR > 0.1 ppb was applied to exclude those retrievals with very weak CH_3OH signals in the TES spectra.

3 Results

3.1 Source characterization of CH_3OH in Mexico outflow

Vertical profiles of CH_3OH and CO mixing ratios from the DC-8 and C-130 during MILAGRO (not shown) indicate outflow mainly at 600–800 hPa near the city center, due to the high elevation of Mexico City. Downwind of the city center, enhanced CH_3OH and CO were detected up to 600 hPa and down to the surface (~1000 hPa), with the

ACPD
12, 5705–5738, 2012

topography leading to a very efficient "air pump" exporting pollutants to the free troposphere (de Foy et al., 2006).

To examine the contributions of various source types to atmospheric CH_3OH during MILAGRO, we examined a suite of gases indicative of anthropogenic, biogenic, and biomass burning sources (the presumed sources of CH_3OH), and their correlations with CH_3OH. These indicator tracers include CO, acetone ($(CH_3)_2CO$), benzene (C_6H_6), acetylene (C_2H_2), hydrogen cyanide (HCN) and acetonitrile (CH_3CN). CO is a general tracer for combustion sources (fossil fuel, biofuel, and biomass burning). Acetone can be a good tracer of biogenic sources due to its relatively long lifetime (Singh et al., 1995). There is also a large source of acetone from atmospheric oxidation of anthropogenic VOCs at northern midlatitudes (Fisher et al., 2012). Benzene can be regarded as an indicator of anthropogenic emissions involving solvent use, vehicle exhaust, and industrial processes (Karl et al., 2009). C_2H_2 is a relatively inert tracer and comes mostly from automobile exhaust (Harley et al., 1992). HCN and CH_3CN are tracers of biomass burning (Singh et al., 2010). Analysis of a subset of C-130 measurements near the MCMA during MILAGRO (Fig. 3) shows that CH_3OH in this outflow region is correlated (1) strongly with CO, acetone and benzene, (2) moderately with C_2H_2, and (3) less with HCN and CH_3CN, suggesting that the main sources of CH_3OH during MILAGRO were anthropogenic and biogenic in nature.

In addition to primary anthropogenic and biogenic sources, photochemical formation could be a contributor to CH_3OH during MILAGRO. As an oxygenated VOC, CH_3OH is produced by reaction of the methylperoxy radical (CH_3O_2) with itself and with other organic peroxy radicals (RO_2) (Tyndall et al., 2001; Madronich and Calvert, 1990). In general, reactions involving CH_3O_2 and RO_2 are not expected to be a large source of CH_3OH in urban environments under high NO_x conditions (Molina et al., 2010). However, the very active photochemical environment and the extremely high RO_2 concentrations in Mexico City could lead to reactions of CH_3O_2 with other peroxy radicals, potentially leading to significant CH_3OH production in this specific region. In addition, Jacob et al. (2005) previously inferred a larger photochemical CH_3OH source than

ACPD
12, 5705–5738, 2012

expected based on present understanding, though in the remote rather than urban polluted atmosphere. Any significant photochemical production of CH_3OH during MILAGRO would have implications for the interpretation of CH_3OH-CO correlations, as will be discussed in Sect. 3.3.

3.2 Spatial variability of CH_3OH and CO concentrations around Mexico City

Figure 4a, b shows the variation in CH_3OH and CO concentrations at 600–800 hPa in the C-130 and DC-8 aircraft observations as a function of distance from the city center. The aircraft observations of both CH_3OH and CO show a decreasing trend with increasing distance away from the urban source region, mainly due to dilution (mixing with background air) and chemical decay.

Figure 4c shows the corresponding variation in the TES CH_3OH RVMR and pseudo CO RVMR. In contrast to the aircraft observations, the TES observations show no decreasing trend with distance downwind of the city. The limited spatial variability in TES CO for this area has been previously reported by Shim et al. (2009), who examined O_3 and CO from TES retrievals and MILAGRO aircraft measurements to characterize mega-city pollution outflow on a regional scale. They found that TES captures much of the spatial and day-to-day variability seen in the in situ data for O_3, but not for CO. In particular, TES does not clearly resolve the CO pollution over the Mexico City Basin. We explored a number of different possible reasons for this lack of spatial variability in TES CO, including sampling issues, the vertical resolution of the TES measurements, and retrieval-related issues associated with the high altitude of Mexico City. Examination of these issues using 5 yr of TES Version 4 CO data over this region led to the conclusion that the handling of the TES Version 4 CO prior constraints over regions with high surface elevation is an important contributor to the inadequate spatial variability in TES CO during MILAGRO. Points within 300 km of the city center mostly have high surface elevation, while areas farther from the center are closer to sea level. For the Version 5 (and previous versions) TES retrievals, the CO constraints are not shifted in altitude for high surface elevation regions. This leads to low values in the constraint

ACPD
12, 5705–5738, 2012

vector and tighter constraints from the prior than are desirable. Therefore, the TES CO values over Mexico City are generally constrained to lower values than they should be due to the a priori constraints. This issue will be considered in future TES algorithm updates. Note that this is less of an issue for the O_3 retrievals, which are far more loosely constrained in the upper troposphere than the CO retrievals. For the CH_3OH retrievals the prior constraints are shifted vertically to account for variations in surface elevation (Cady-Pereira et al., 2012).

An additional contributor to the lack of spatial variability in CH_3OH and CO during MILAGRO is the coarse vertical resolution of the measurements. In situ outflow profiles measured during MILAGRO show concentrations that peak in a relatively narrow range. The TES CH_3OH and CO retrievals are unable to distinguish between profiles with a sharp, strongly enhanced peak, and profiles where the trace gas enhancement has lower peak values but is spread over a wider vertical range. Therefore, TES does not reproduce the extreme high peak values observed by the aircraft, and would be expected to show lower average values than the plume-chasing aircraft, particularly in the region closest to the city center. However, this is not expected to bias the derived CH_3OH-CO correlation.

3.3 Impact of vertical resolution of TES retrieval on the derived $\Delta CH_3OH/\Delta CO$ ratio

In this study the CH_3OH/CO enhancement ratio is defined as the slope of the regression between CH_3OH and CO, and is denoted as $\Delta CH_3OH/\Delta CO$. The slope is calculated using the reduced major axis (RMA) method, which estimates the linear relationship between two variables by minimizing the residual variance in both x and y directions (Xiao et al., 2004; Hirsch and Gilroy, 1984). For the aircraft in-situ measurements, it is straightforward to derive $\Delta CH_3OH/\Delta CO$. For the TES observations, the $\Delta CH_3OH/\Delta CO$ ratio is the regression slope between the CH_3OH RVMR and the pseudo CO RVMR (see Sect. 2.2).

ACPD
12, 5705–5738, 2012

The vertical resolution of the TES measurement should be taken into consideration for the interpretation of the retrieved CH_3OH and CO and the associated spatial variability in Mexico City outflow. Simulated retrievals are utilized to examine whether the coarse vertical resolution of TES CH_3OH and CO observations would be expected to affect the derived $\Delta CH_3OH/\Delta CO$ ratios.

Starting with averaged C-130 aircraft profiles of CH_3OH and CO near the Mexico City center (<300 km), we constructed a base profile for each species, which was then scaled by factors of 1.25, 1.5 and 1.75 to create four profiles in total. These four profiles (shown as dashed lines in Fig. 5a and b) were used as "truth" to generate four sets of simulated TES radiances. Realistic noise was included in the simulated radiances. CH_3OH retrievals were then performed on the simulated radiances. Simulated CO retrievals were generated from the assumed "true" profiles by applying the a priori and averaging kernel from a typical TES case with relatively strong sensitivity (from Version 4 of the TES operational algorithm). Retrieved profiles are shown as solid lines in Fig. 5a and b. Thus, for each set of CH_3OH and CO retrieved profiles, we have a pair of CH_3OH and CO RVMRs, resulting in the TES $\Delta CH_3OH/\Delta CO$ ratio shown in Fig. 5d. Despite the coarse vertical resolution of the TES measurements, TES is able to recover the true $\Delta CH_3OH/\Delta CO$ ratio when both CH_3OH and CO retrievals show relatively high sensitivity.

3.4 Spatial variability in the $\Delta CH_3OH/\Delta CO$ ratio

In order to explore the utility of CH_3OH-CO correlations from TES observations, we evaluated the extent to which variability in the CH_3OH/CO enhancement ratio is captured by TES based on in-situ aircraft observations during MILAGRO. The $\Delta CH_3OH/\Delta CO$ ratio observed by TES reflects the bulk enhancements of CH_3OH and CO in the Mexico City outflow, smoothed by the TES vertical sensitivity. For TES/aircraft comparisons of the $\Delta CH_3OH/\Delta CO$ ratio, only aircraft data in the 600–800 hPa range, the region where the TES CH_3OH and CO retrievals have the greatest sensitivity, are used.

ACPD
12, 5705–5738, 2012

Figure 6a shows the CH_3OH-CO correlations from the two aircraft. In contrast with the CH_3OH and CO concentrations themselves, $\Delta CH_3OH/\Delta CO$ ratios for air masses with significant source influence vary little with geographical location. Instead, slightly higher ratios are seen outside the 300 km range as compared to within 300 km around the city. This may be explained by photochemical production of CH_3OH. The $\Delta CH_3OH/\Delta CO$ ratios based on the C-130 aircraft measurements are 41–55 ppt ppb^{-1}, while the DC-8 observations show much lower values of 26–39 ppt ppb^{-1}. The different $\Delta CH_3OH/\Delta CO$ ratios between the C-130 and DC-8 measurements appear to reflect a calibration offset (see Sect. 2.1) rather than the different sampling strategy for the two aircraft (Singh et al., 2009), since the discrepancy persists regardless of the distance from the MCMA (Fig. 6a).

Figure 6b shows the corresponding CH_3OH-CO correlations as measured by TES. As with the aircraft observations (Fig. 6a), TES $\Delta CH_3OH/\Delta CO$ ratios display little variation with distance from the city center (ranging from 18 to 24 ppt ppb^{-1}), and are closer to the values derived from the DC-8 measurements during MILAGRO than to those derived from the C-130 measurements. Note that close to Mexico City center, we expect TES CO retrievals using the Version 4 algorithm to under-represent the true values due to the issues with the constraints discussed above. This particular issue should not be present in the TES CH_3OH observations as our retrieval shifts the constraints. With more appropriate CO constraints, it is expected that the TES data will exhibit some spatial variation in the enhancement ratios, with slightly lower ratio values (increased CO values) closer to the city center, as seen in the aircraft data.

Any discrepancies between TES and aircraft ratios for the MILAGRO dataset may be due to aircraft instrument calibration issues, or to systematic errors in the TES results. Possible sources of systematic error in the TES retrievals include forward model errors (such as biases in spectroscopic line parameters or incorrect representation of interfering species), errors in the TES radiance calibration, and influence of the a priori assumptions in the retrieval (the effect of the a priori assumptions is mitigated, but not eliminated, by the RVMR representation). Given the present discrepancy between the

ACPD
12, 5705–5738, 2012

aircraft measurements of CH_3OH, it is difficult at this stage to use the aircraft observations as evaluation of the absolute TES enhancement ratios.

In contrast with Mexico City, a region dominated by strong anthropogenic emissions, we also examine the TES $\Delta CH_3OH/\Delta CO$ ratios over the Amazon Basin, a region dominated by biogenic emissions (with an additional biomass burning source contribution) (Karl et al., 2007). Similar to the MILAGRO domain the Amazon region exhibits elevated CH_3OH values, which provides a relatively high signal-to-noise ratio for the TES observations. Figure 7 shows TES $\Delta CH_3OH/\Delta CO$ ratios over the Amazon Basin during August–September of 2005. The ratio of 42 ± 7 ppt ppb^{-1} is a factor of 2 higher than that observed near Mexico City during MILAGRO (18–24 ppt ppb^{-1}). The significant ratio difference between Mexico City and the Amazon Basin indicates that the TES-derived $\Delta CH_3OH/\Delta CO$ ratio has potential for differentiating source categories of CH_3OH and other chemical species with multiple sources (e.g. CO_2). With future work, the TES-derived ratio could be applied globally to other regions and time periods where no in situ measurements are available.

It should be noted that connecting the observed $\Delta CH_3OH/\Delta CO$ ratio from either aircraft or TES with the actual CH_3OH/CO emission ratio from "urban" sources in Mexico City is complicated, since the $\Delta CH_3OH/\Delta CO$ ratio could have already been enhanced due to photochemical production of CH_3OH even in the plumes thought to be "fresh". Ground-based estimates of emission ratios tend to show lower values than the enhancement ratios measured aboard aircraft. For example, Bon et al. (2011) report CH_3OH/CO emission ratios of 2.1 ± 0.5 ppt ppb^{-1} and 6.1 ± 2.1 ppt ppb^{-1} from boundary layer observations at urban sites during MILAGRO. The complicated relationship between emission ratios at the source and enhancement ratios in plumes does not apply just too urban sources. For instance, Holzinger et al. (2005) observed relatively high CH_3OH and acetone enhancements in fire plumes over the Mediterranean, and concluded that secondary production of these species must have taken place. Caution is therefore needed when interpreting enhancement ratios as opposed to emission ratios.

ACPD
12, 5705–5738, 2012

3.5 $\Delta CH_3OH/\Delta CO$ ratio from other campaigns

The $\Delta CH_3OH/\Delta CO$ ratios derived in this analysis from the C-130 observations during MILAGRO (41–55 ppt ppb^{-1}) are significantly higher than ratios from other aircraft studies in US cities (Table 1). Singh et al. (2010) derived a ratio of 21.0 ± 14.0 ppb ppb^{-1} in urban plumes mainly sampled over California. Warneke et al. (2007) derived a ratio of 9 ppt ppb^{-1} in fresh New York City and Boston plumes in July and August of 2004, and 8.4 ppt ppb^{-1} from aircraft observations over the Los Angeles Basin in the spring of 2002. The ratios from the C-130 measurements during MILAGRO are also much higher than the ratios of 4–11 ppt ppb^{-1} over Boulder, Colorado and Pittsburgh, Pennsylvania reported from ground-based winter measurements (Millet et al., 2005; Goldan et al., 1995).

To put these urban values into context, $\Delta CH_3OH/\Delta CO$ ratios have also been reported for biomass burning plumes during the MILAGRO experiment. High ratios of 14–28 ppt ppb^{-1} were reported by Yokelson et al. (2009) based on aircraft measurements of fresh plumes from fires in the Yucatan region of Mexico. Comparable ratios of 19–32 ppt ppb^{-1} can be derived from the data presented by Yokelson et al. (2011), who reported emission factors for 25 open fires based on airborne measurements during March 2006.

The aircraft $\Delta CH_3OH/\Delta CO$ ratios from Mexico City are also much higher than those reported from biomass burning at northern mid/high latitudes. Simpson et al. (2011) and Singh et al. (2010) derived mean ratios of 9.6 ± 1.9 ppt ppb^{-1}, and 15.6 ± 9.2 ppb ppb^{-1}, respectively, in fresh Canadian fire plumes. De Gouw et al. (2006) derived a ratio of 10.8 ± 4.4 ppt ppb^{-1} from aged fire plumes in Alaska and Western Canada. Goode et al. (2000) derived a ratio of 14 ± 1 ppt ppb^{-1} for forest fire plumes in Alaska.

ACPD
12, 5705–5738, 2012

4 Conclusions

The correlation between CH_3OH and carbon monoxide (CO) is of interest for characterizing sources of CH_3OH and other species. Coincident measurements of CH_3OH and CO in the lower to middle troposphere from TES and aircraft observations during MILAGRO allowed us to assess the utility of satellite-based observations of the CH_3OH-CO correlation.

TES retrievals of CH_3OH and CO show relatively high sensitivity in the 600–800 hPa range, where Mexico City pollution outflow peaks. In-situ aircraft observations of CH_3OH and CO downwind of Mexico City center during MILAGRO in March 2006 were used to evaluate the extent to which variability in the $\Delta CH_3OH/\Delta CO$ enhancement ratio is captured by TES special observations. During MILAGRO there are sharply peaked outflow profiles (from shallow plumes) that are particularly challenging for TES (or any nadir satellite measurements) to capture due to its vertical resolution ($\sim$ 5 km). The analysis suggests that the TES operational CO retrieval algorithm (Version 5) maybe improved in regions of elevated topography (e.g. Mexico City) by updating algorithm CO constraints to better handle elevation changes.

$\Delta CH_3OH/\Delta CO$ ratios derived from the TES observations reflect bulk enhancements (smoothed according to the TES sensitivity) of CH_3OH and CO in the Mexico City outflow. $\Delta CH_3OH/\Delta CO$ ratios derived from the TES observations (18–24 ppt ppb^{-1}) are closer to those observed from DC-8 aircraft during MILAGRO (26–39 ppt ppb^{-1}), than those from C-130 observations (41–55 ppt ppb^{-1}). In a test case of simulated TES CH_3OH and CO retrievals with relatively high sensitivity, TES is able to reproduce the $\Delta CH_3OH/\Delta CO$ correlation in spite of the coarse vertical resolution of the retrievals. A discrepancy in observed $\Delta CH_3OH/\Delta CO$ ratios between the TES and aircraft data could be due to a number of possible systematic errors, including aircraft instrument calibration, TES radiance calibration, TES forward model errors and influence of the a priori constraints on the TES retrievals. The apparent offset between the different aircraft measurements precludes a direct validation of the TES-derived CH_3OH:CO

ACPD
12, 5705–5738, 2012

ratios for this analysis. However, the CH_3OH/CO enhancement ratios derived from the TES and aircraft data during MILAGRO are both high relative to previous studies over US cities. This may be partly explained by photochemical production of CH_3OH in fresh plumes as well as to the different types of fuel burned in the MCMA.

TES derived $\Delta CH_3OH/\Delta CO$ ratios show a significant difference between Mexico City and the Amazon Basin, with substantially higher ratios over the Amazon. Both regions feature strong CH_3OH emissions: from anthropogenic sources in the first case and from biogenic sources in the second. This analysis shows that TES can clearly distinguish differences in the $\Delta CH_3OH/\Delta CO$ ratio due to two different source categories of CH_3OH, which indicates the potential of utilizing TES derived ratios globally as a diagnostic for emission sources in other regions and time periods.

Acknowledgements. This work was supported by NASA through the Atmospheric Chemistry Modeling and Analysis Program (Grant #NNX10AG65G). Research was partially supported by the Jet Propulsion Laboratory, California Institute of Technology under contract to the National Aeronautics and Space Administration (NASA). We also thank John Worden at NASA/JPL for helpful discussions. We acknowledge Don Blake at University of California, Irvine and Paul Wennberg at California Institute of Technology for sharing their measurements.

References

Apel, E. C., Emmons, L. K., Karl, T., Flocke, F., Hills, A. J., Madronich, S., Lee-Taylor, J., Fried, A., Weibring, P., Walega, J., Richter, D., Tie, X., Mauldin, L., Campos, T., Weinheimer, A., Knapp, D., Sive, B., Kleinman, L., Springston, S., Zaveri, R., Ortega, J., Voss, P., Blake, D., Baker, A., Warneke, C., Welsh-Bon, D., de Gouw, J., Zheng, J., Zhang, R., Rudolph, J., Junkermann, W., and Riemer, D. D.: Chemical evolution of volatile organic compounds in the outflow of the Mexico City Metropolitan area, Atmos. Chem. Phys., 10, 2353–2375, doi:10.5194/acp-10-2353-2010, 2010.

Alvarado, M. J., Cady-Pereira, K. E., Xiao, Y., Millet, D. B., and Payne, V. H.: Emission Ratios for Ammonia and Formic Acid and Observations of Peroxy Acetyl Nitrate (PAN) and Ethylene

ACPD

12, 5705–5738, 2012

in Biomass Burning Smoke as Seen by the Tropospheric Emission Spectrometer (TES), Atmosphere, 2, 633–654, 2011.
Beer, R., Glavich, T. A., and Rider, D. M.: Tropospheric emission spectrometer for the Earth Observing System's Aura Satellite, Appl. Opt., 40, 2356–2367, 2001.
Beer, R., Shephard, M. W., Kulawik, S. S., Clough, S. A., Eldering, A., Bowman, K. W., Sander, S. P., Fisher, B. M., Payne, V. H., Luo, M., Osterman, G. B., and Worden, J. R.: First satellite observations of lower tropospheric ammonia and methanol, Geophys. Res. Lett., 35, L09801, doi:10.1029/2008GL033642, 2008.
Blake, D. R. and Rowland, F. S.: Urban Leakage of Liquefied Petroleum Gas and Its Impact on Mexico-City Air-Quality, Science, 269, 953–956, 1995.
Blando, J. D. and Turpin, B. J.: "Secondary organic aerosol formation in cloud and fog droplets: a literature evaluation of plausibility", Atmos. Environ., 34, 1623–1632, 2000.
Bon, D. M., Ulbrich, I. M., de Gouw, J. A., Warneke, C., Kuster, W. C., Alexander, M. L., Baker, A., Beyersdorf, A. J., Blake, D., Fall, R., Jimenez, J. L., Herndon, S. C., Huey, L. G., Knighton, W. B., Ortega, J., Springston, S., and Vargas, O.: Measurements of volatile organic compounds at a suburban ground site (T1) in Mexico City during the MILAGRO 2006 campaign: measurement comparison, emission ratios, and source attribution, Atmos. Chem. Phys., 11, 2399–2421, doi:10.5194/acp-11-2399-2011, 2011.
Cady-Pereira, K. E., Shephard, M. W., Millet, D. B., Xiao, Y., Luo, M., Wells, K. C., Payne V. H., and Worden, J.: Methanol from Space: Retrieval Strategy and Seasonal and Spatial Variability from TES Global Observations, in preparation, 2012.
Coheur, P.-F., Herbin, H., Clerbaux, C., Hurtmans, D., Wespes, C., Carleer, M., Turquety, S., Rinsland, C. P., Remedios, J., Hauglustaine, D., Boone, C. D., and Bernath, P. F.: ACE-FTS observation of a young biomass burning plume: first reported measurements of C_2H_4, C_3H_6O, H_2CO and PAN by infrared occultation from space, Atmos. Chem. Phys., 7, 5437–5446, doi:10.5194/acp-7-5437-2007, 2007.
Connor, T. C., Shephard, M. W., Payne, V. H., Cady-Pereira, K. E., Kulawik, S. S., Luo, M., Osterman, G., and Lampel, M.: Long-term stability of TES satellite radiance measurements, Atmos. Meas. Tech., 4, 1481–1490, doi:10.5194/amt-4-1481-2011, 2011.
Crounse, J. D., DeCarlo, P. F., Blake, D. R., Emmons, L. K., Campos, T. L., Apel, E. C., Clarke, A. D., Weinheimer, A. J., McCabe, D. C., Yokelson, R. J., Jimenez, J. L., and Wennberg, P. O.: Biomass burning and urban air pollution over the Central Mexican Plateau, Atmos. Chem. Phys., 9, 4929–4944, doi:10.5194/acp-9-4929-2009, 2009.

ACPD
12, 5705–5738, 2012

de Gouw, J. A., Middlebrook, A. M., Warneke, C., Goldan, P. D., Kuster, W. C., Roberts, J. M., Fehsenfeld, F. C., Worsnop, D. R., Canagaratna, M. R., Pszenny, A. A. P., Keene, W. C., Marchewka, M., Bertman, S. B., and Bates, T. S.: Budget of organic carbon in a polluted atmosphere: Results from the New England Air Quality Study in 2002, J. Geophys. Res., 110, D16305, doi:10.1029/2004JD005623, 2005.

de Gouw, J. A., Warneke, C., Stohl, A., Wollny, A. G., Brock, C. A., Cooper, O. R., Holloway, J. S., Trainer, M., Fehsenfeld, F. C., Atlas, E. L., Donnelly, S. G., Stroud, V., and Lueb, A.: Volatile organic compounds composition of merged and aged forest fire plumes from Alaska and western Canada, J. Geophys. Res., 111, D10303, doi:10.1029/2005JD006175, 2006.

de Gouw, J. A., Welsh-Bon, D., Warneke, C., Kuster, W. C., Alexander, L., Baker, A. K., Beyersdorf, A. J., Blake, D. R., Canagaratna, M., Celada, A. T., Huey, L. G., Junkermann, W., Onasch, T. B., Salcido, A., Sjostedt, S. J., Sullivan, A. P., Tanner, D. J., Vargas, O., Weber, R. J., Worsnop, D. R., Yu, X. Y., and Zaveri, R.: Emission and chemistry of organic carbon in the gas and aerosol phase at a sub-urban site near Mexico City in March 2006 during the MILAGRO study, Atmos. Chem. Phys., 9, 3425–3442, doi:10.5194/acp-9-3425-2009, 2009.

de Foy, B., Varela, J. R., Molina, L. T., and Molina, M. J.: Rapid ventilation of the Mexico City basin and regional fate of the urban plume, Atmos. Chem. Phys., 6, 2321–2335, doi:10.5194/acp-6-2321-2006, 2006.

Dufour, G., Boone, C. D., Rinsland, C. P., and Bernath, P. F.: First space-borne measurements of methanol inside aged southern tropical to mid-latitude biomass burning plumes using the ACE-FTS instrument, Atmos. Chem. Phys., 6, 3463–3470, doi:10.5194/acp-6-3463-2006, 2006.

Duncan, B. N., Logan, J. A., Bey, I., Megretskaia, I. A., Yantosca, R. M., Novelli, P. C., Jones, N. B., and Rinsland, C. P.: Global budget of CO, 1988–1997: Source estimates and validation with a global model, J. Geophys. Res., 112, D22301, doi:10.1029/2007jd008459, 2007.

Fischer, E. V., Jacob, D. J., Millet, D. B., Yantosca, R. M., and Mao, J.: The role of the ocean in the global atmospheric budget of acetone, Geophys. Res. Lett., 39, L01807, doi:10.1029/2011GL050086, 2012.

Galbally, I. E. and Kirstine, W.: The production of methanol by flowering plants and the global cycle of methanol, J. Atmos. Chem., 43, 195–229, 2002.

Goldan, P. D., Trainer, M., Kuster, W. C., Parrish, D. D., Carpenter, J., Roberts, J. M., Yee, J. E., and Fehsenfeld, F. C.: Measurements of hydrocarbons, oxygenated hydrocarbons, carbonmonoxide, and nitrogen-oxides in an urban basin in Colorado – Implications for emissions

ACPD
12, 5705–5738, 2012

inventories, J. Geophys. Res., 100, 22771–22783, 1995.
Goode, J. G., Yokelson, R. J., Ward, D. E., Susott, R. A., Babbitt, R. E., Davies, M. A., and Hao, W. M.: Measurements of excess O_3, CO_2, CO, CH_4, C_2H_4, C_2H_2, HCN, NO NH_3, HCOOH, CH_3COOH, HCHO and CH_3OH in 1997 Alaskan biomass burning plumes by airborne Fourier transform infrared spectroscopy (AFTIR), J. Geophys. Res., 105, 22147–22166, 2000.
Harley, P., Greenberg, J., Niinemets, ., and Guenther, A.: Environmental controls over methanol emission from leaves, Biogeosciences, 4, 1083–1099, doi:10.5194/bg-4-1083-2007, 2007.
Harley, R. A., Hannigan, M. P., and Cass, G. R.: Respeciation of organic gas emissions and the detection of excess unburned gasoline in the atmosphere, Environ. Sci. Technol., 26, 2395–2408, doi:10.1021/es00036a010, 1992.
Heikes, B. G., Chang, W., Pilson, M. E. Q., Swift, E., Singh, H. B., Guenther, A., Jacob, D. J., and Brand, L.: Atmospheric methanol budget and ocean implication, Global Biogeochem. Cy., 16, 1133, doi:10.1029/2002GB001895, 2002.
Hirsch, R. M. and Gilroy, E. J.: Methods of fitting a straight line to data: Examples in water resources, Water Resour. Bull., 20, 705–711, 1984.
Holloway, J. S., Jakoubek, R. O., Parrish, D. D., Gerbig, C., Volz-Thomas, A., Schmitgen, S., Fried, A., Wert, B., Henry, B., and Drummond, J. R.: Airborne intercomparison of vacuum ultraviolet fluorescence and tunable diode laser absorption measurements of tropospheric carbon monoxide, J. Geophys. Res., 105, 24251–24261, 2000.
Holzinger, R., Williams, J., Salisbury, G., Klüpfel, T., de Reus, M., Traub, M., Crutzen, P. J., and Lelieveld, J.: Oxygenated compounds in aged biomass burning plumes over the Eastern Mediterranean: evidence for strong secondary production of methanol and acetone, Atmos. Chem. Phys., 5, 39–46, doi:10.5194/acp-5-39-2005, 2005.
Hu, L., Millet, D. B., Mohr, M. J., Wells, K. C., Griffis, T. J., and Helmig, D.: Sources and seasonality of atmospheric methanol based on tall tower measurements in the US Upper Midwest, Atmos. Chem. Phys., 11, 11145–11156, doi:10.5194/acp-11-11145-2011, 2011.
Jacob, D. J., Field, B. D., Li, Q. B., Blake, D. R., de Gouw, J., Warneke, C., Hansel, A., Wisthaler, A., Singh, H. B., and Guenther, A.: Global budget of methanol: Constraints from atmospheric observations, J. Geophys. Res., 110, D08303, doi:10.1029/2004JD005172, 2005
Karl, T., Guenther, A., Spirig, C., Hansel, A., and Fall, R.: Seasonal variation of biogenic VOC emissions above a mixed hardwood forest in Northern Michigan, Geophys. Res. Lett., 30, 2186, doi:10.1029/2003GL018432, 2003.
Karl, T., Guenther, A., Yokelson, R. J., Greenberg, J., Potosnak, M., Blake, D. R., and Artaxo,

ACPD
12, 5705–5738, 2012

P.: The tropical forest and fire emissions experiment: Emission, chemistry, and transport of biogenic volatile organic compounds in the lower atmosphere over Amazonia, J. Geophys. Res.-Atmos., 112, D18302, doi:10.1029/2007jd008539, 2007.

Karl, T., Apel, E., Hodzic, A., Riemer, D. D., Blake, D. R., and Wiedinmyer, C.: Emissions of volatile organic compounds inferred from airborne flux measurements over a megacity, Atmos. Chem. Phys., 9, 271–285, doi:10.5194/acp-9-271-2009, 2009

Karl, T., Harley, P., Emmons, L., Thornton, B., Guenther, A., Basu, C., Turnipseed, A., and Jardine, K.: Efficient Atmospheric Cleansing of Oxidized Organic Trace Gases by Vegetation, Science, 330, 816–819, 2010.

Kleb, M. M., Chen, G., Crawford, J. H., Flocke, F. M., and Brown, C. C.: An overview of measurement comparisons from the INTEX-B/MILAGRO airborne field campaign, Atmos. Meas. Tech., 4, 9–27, doi:10.5194/amt-4-9-2011, 2011.

Lopez, J. P., Luo, M., Christensen, L. E., Loewenstein, M., Jost, H., Webster, C. R., and Osterman, G.: TES carbon monoxide validation during two AVE campaigns using the Argus and ALIAS instruments on NASA's WB-57F, J. Geophys. Res., 113, D16S47, doi:10.1029/2007JD008811, 2008.

Luo, M., Rinsland, C. P., Rodgers, C. D., Logan, J. A., Worden, H., Kulawik, S., Eldering, A., Goldman, A., Shephard, M. W., Gunson, M., and Lampel, M.: Comparison of carbon monoxide measurements by TES and MOPITT: Influence of a priori data and instrument characteristics on nadir atmospheric species retrievals, J. Geophys. Res., 112, D09303, doi:10.1029/2006JD007663, 2007a.

Luo, M., Rinsland, C., Fisher, B., Sachse, G., Diskin, G., Logan, J., Worden, H., Kulawik, S., Osterman, G., Eldering, A., Herman, R., and Shephard, M.: TES carbon monoxide validation with DACOM aircraft measurements during INTEX-B 2006, J. Geophys. Res., 112, D24S48, doi:10.1029/2007JD008803, 2007b.

Madronich, S. and Calvert, J. G.: Permutation reactions of organic peroxy radicals in the troposphere, J. Geophys. Res., 95, 5697–5715, 1990.

Millet, D. B., Jacob, D. J., Turquety, S., Hudman, R. C., Wu, S., Fried, A., Walega, J., Heikes, B. G., Blake, D. R., Singh, H. B., Anderson, B. E., and Clarke, A. D.: Formaldehyde distribution over North America: Implications for satellite retrievals of formaldehyde columns and isoprene emission, J. Geosphys. Res., 111, D24S02, doi:10.1029/2005jd006853, 2006.

Millet, D. B., Jacob, D. J., Custer, T. G., de Gouw, J. A., Goldstein, A. H., Karl, T., Singh, H. B., Sive, B. C., Talbot, R. W., Warneke, C., and Williams, J.: New constraints on terres-

ACPD
12, 5705–5738, 2012

trial and oceanic sources of atmospheric methanol, Atmos. Chem. Phys., 8, 6887–6905, doi:10.5194/acp-8-6887-2008, 2008.
Molina, L. T., Madronich, S., Gaffney, J. S., Apel, E., de Foy, B., Fast, J., Ferrare, R., Herndon, S., Jimenez, J. L., Lamb, B., Osornio-Vargas, A. R., Russell, P., Schauer, J. J., Stevens, P. S., Volkamer, R., and Zavala, M.: An overview of the MILAGRO 2006 Campaign: Mexico City emissions and their transport and transformation, Atmos. Chem. Phys., 10, 8697–8760, doi:10.5194/acp-10-8697-2010, 2010.
Payne, V. H., Clough, S. A., Shephard, M. W., Nassar, R., and Logan, J. A.: Information-centered representation of retrievals with limited degrees of freedom for signal: Application to methane from the Tropospheric Emission Spectrometer, J. Geophys. Res., 114, D10307, doi:10.1029/2008jd010155, 2009.
Paton-Walsh, C., Wilson, S. R., Jones, N. B., and Griffith, D. W. T.: Measurement of methanol emissions from Australian wildfires by ground-based solar Fourier transform spectroscopy, Geophys. Res. Lett., 35, L08810, doi:10.1029/2007GL032951, 2008.
Razavi, A., Karagulian, F., Clarisse, L., Hurtmans, D., Coheur, P. F., Clerbaux, C., Müller, J. F., and Stavrakou, T.: Global distributions of methanol and formic acid retrieved for the first time from the IASI/MetOp thermal infrared sounder, Atmos. Chem. Phys., 11, 857–872, doi:10.5194/acp-11-857-2011, 2011.
Rinsland, C. P., Mahieu, E., Chiou, L., and Herbin, H.: First ground-based infrared solar absorption measurements of free tropospheric methanol (CH_3OH): Multidecade infrared time series from Kitt Peak (31.9° N 111.6° W): Trend, seasonal cycle, and comparison with previous measurements, J. Geophys. Res., 114, D04309, doi:10.1029/2008JD011003, 2009.
Sachse, G. W., Hill, G. F., Wade, L. O., and Perry, M. G.: Fastresponse, high-precision carbon monoxide sensor using a tunable diode-laser absorption technique, J. Geophys. Res., 92, 2071–2081, 1987.
Shephard, M. W., Worden, H. M., Cady-Pereira, K. E., Lampel, M., Luo, M., Bowman, K. W., Sarkissian, E., Beer, R., Rider, D. M., Tobin, D. C., Revercomb, H. E., Fisher, B. M., Tremblay, D., Clough, S. A., Osterman, G. B., and Gunson, M.: Tropospheric Emission Spectrometer Spectral Radiance Comparisons, J. Geophys. Res., 113, D15S05, doi:10.1029/2007JD008856, 2008.
Shephard, M. W., Cady-Pereira, K. E., Luo, M., Henze, D. K., Pinder, R. W., Walker, J. T., Rinsland, C. P., Bash, J. O., Zhu, L., Payne, V. H., and Clarisse, L.: TES ammonia retrieval strategy and global observations of the spatial and seasonal variability of ammonia, Atmos.

ACPD
12, 5705–5738, 2012

Chem. Phys., 11, 10743–10763, doi:10.5194/acp-11-10743-2011, 2011.
Shim, C., Li, Q., Luo, M., Kulawik, S., Worden, H., Worden, J., Eldering, A., Diskin, G., Sachse, G., Weinheimer, A., Knapp, D., Montzca, D., and Campos, T.: Satellite observations of Mexico City pollution outflow from the Tropospheric Emissions Spectrometer (TES), Atmos. Environ., 43, 1540–1547, doi:10.1016/j.atmosenv.2008.11.026, 2009.
Simpson, I. J., Akagi, S. K., Barletta, B., Blake, N. J., Choi, Y., Diskin, G. S., Fried, A., Fuelberg, H. E., Meinardi, S., Rowland, F. S., Vay, S. A., Weinheimer, A. J., Wennberg, P. O., Wiebring, P., Wisthaler, A., Yang, M., Yokelson, R. J., and Blake, D. R.: Boreal forest fire emissions in fresh Canadian smoke plumes: C1–C10 volatile organic compounds (VOCs), CO_2, CO, NO_2, NO, HCN and CH_3CN, Atmos. Chem. Phys., 11, 6445–6463, doi:10.5194/acp-11-6445-2011, 2011.
Singh, H. B., Kanakidou, M., Crutzen P. J., and Jacob, D. J.: High-Concentrations and Photochemical Fate of Oxygenated Hydrocarbons in the Global Troposphere, Nature, 378, 50–54, 6552, doi:10.1038/378050a0, 1995.
Singh, H. B., Tabazadeh, A., Fukui, Y., Bey, I., Yantosca, R., Jacob, D., Arnold, F., Wohlfrom K., Atlas, E., Flocke, F., Blake, D., Blake, N., Heikes, B., Snow, J., Talbot, R., Gregory, G., Sachse, G., Vay, S., and Kondo, Y.: Distribution and fate of selected oxygenated organic species in the troposphere and lower stratosphere over the Atlantic, J. Geophys. Res., 105, 3795–3805, 2000.
Singh, H. B., Salas, L. J., Chatfield, R. B., Czech, E., Fried, A., Walega, J., Evans, M. J., Field, B. D., Jacob, D. J., Blake, D., Heikes, B., Talbot, R., Sachse, G., Crawford, J. H., Avery, M. A., Sandholm, S., and Fuelberg, H.: Analysis of the atmospheric distribution, sources, and sinks of oxygenated volatile organic chemicals based on measurements over the Pacific during TRACE-P, J. Geophys. Res., 109, D15S07, doi:10.1029/2003JD003883, 2004.
Singh, H. B., Brune, W. H., Crawford, J. H., Flocke, F., and Jacob, D. J.: Chemistry and transport of pollution over the Gulf of Mexico and the Pacific: spring 2006 INTEX-B campaign overview and first results, Atmos. Chem. Phys., 9, 2301–2318, doi:10.5194/acp-9-2301-2009, 2009.
Singh, H. B., Anderson, B. E., Brune, W. H., Cai, C., Cohen, R. C., Crawford, J. H., Cubison, M. J., Czech, E. P., Emmons, L., Fuelberg, H. E., Huey, G., Jacob, D. J., Jimenez, J. L., Kaduwela, A., Kondo, Y., Mao, J., Olson, J. R., Sachse, G. W., Vay, S. A., Weinheimer, A., Wennberg, P. O., Wisthaler, A., and the ARCTAS Science Team: Pollution influences on atmospheric composition and chemistry at high northern latitudes: Boreal and California forest fire emissions, Atmos. Environ., 44, 4553–4564, doi:10.1016/j.atmosenv.2010.08.026,

ACPD
12, 5705–5738, 2012

2010.
Stavrakou, T., Guenther, A., Razavi, A., Clarisse, L., Clerbaux, C., Coheur, P.-F., Hurtmans, D., Karagulian, F., De Mazière, M., Vigouroux, C., Amelynck, C., Schoon, N., Laffineur, Q., Heinesch, B., Aubinet, M., Rinsland, C., and Müller, J.-F.: First space-based derivation of the global atmospheric methanol emission fluxes, Atmos. Chem. Phys., 11, 4873–4898, doi:10.5194/acp-11-4873-2011, 2011.
Tie, X., Guenther, A., and Holland, E.: Biogenic methanol and its impacts on tropospheric oxidants, Geophys. Res. Lett., 30, 1881, doi:10.1029/2003GL017167, 2003.
Tyndall, G. S., Cox, R. A., Granier, C., Lesclaux, R., Moortgat, G. K., Pilling, M. J., Ravishankara, A. R., and Wallington, T. J.: Atmospheric chemistry of small organic peroxy radicals, J. Geophys. Res., 106, 12157–12182, 2001.
Warneke, C., Karl, T., Judmaier, H., Hansel, A., Jordan, A., Lindinger, W., and Crutzen, P. J.: Acetone, methanol, and other partially oxidized volatile organic emissions from dead plant matter by abiological processes: Significance for atmospheric HOx chemistry, Global Biogeochem. Cy., 13, 9–17, doi:10.1029/98gb02428, 1999.
Warneke, C., McKeen, S. A., de Gouw, J. A., Goldan, P. D., Kuster, W. C., Holloway, J. S., Williams, E. J., Lerner, B. M., Parrish, D. D., Trainer, M., Fehsenfeld, F. C., Kato, S., Atlas, E. L., Baker, A., and Blake, D. R.: Determination of urban volatile organic compound emission ratios and comparison with an emissions database, J. Geophys. Res., 112, D10S47, doi:10.1029/2006JD007930, 2007.
Wells K., Millet, D., Cady-Pereira, K., Shephard, M., Xiao, Y., Razavi, A., Clerbaux, C., Clarisse, L., Coheur, P. F., E. Apel, de Gouw, J., Warneke, C., Singh, H., Goldstein, A., Hu, L., and Sive, B.: Tropospheric methanol observations from space: Retrieval evaluation and constraints on the seasonality of biogenic emissions, Atmos. Chem. Phys., in press, 2012.
Xiao, Y. P., Jacob, D. J., Wang, J. S., Logan, J. A., Palmer, P. I., Suntharalingam, P., Yantosca, R. M., Sachse, G. W., Blake, D. R., and Streets, D. G.: Constraints on Asian and European sources of methane from CH_4-C_2H_6-CO correlations in Asian outflow, J. Geophys. Res., 109, D15S16, doi:10.1029/2003JD004475, 2004
Yokelson, R. J., Urbanski, S. P., Atlas, E. L., Toohey, D. W., Alvarado, E. C., Crounse, J. D., Wennberg, P. O., Fisher, M. E., Wold, C. E., Campos, T. L., Adachi, K., Buseck, P. R., and Hao, W. M.: Emissions from forest fires near Mexico City, Atmos. Chem. Phys., 7, 5569–5584, doi:10.5194/acp-7-5569-2007, 2007.
Yokelson, R. J., Crounse, J. D., DeCarlo, P. F., Karl, T., Urbanski, S., Atlas, E., Campos, T.,

ACPD
12, 5705–5738, 2012

Shinozuka, Y., Kapustin, V., Clarke, A. D., Weinheimer, A., Knapp, D. J., Montzka, D. D., Holloway, J., Weibring, P., Flocke, F., Zheng, W., Toohey, D., Wennberg, P. O., Wiedinmyer, C., Mauldin, L., Fried, A., Richter, D., Walega, J., Jimenez, J. L., Adachi, K., Buseck, P. R., Hall, S. R., and Shetter, R.: Emissions from biomass burning in the Yucatan, Atmos. Chem. Phys., 9, 5785–5812, doi:10.5194/acp-9-5785-2009, 2009.

Yokelson, R. J., Burling, I. R., Urbanski, S. P., Atlas, E. L., Adachi, K., Buseck, P. R., Wiedinmyer, C., Akagi, S. K., Toohey, D. W., and Wold, C. E.: Trace gas and particle emissions from open biomass burning in Mexico, Atmos. Chem. Phys., 11, 6787–6808, doi:10.5194/acp-11-6787-2011, 2011.

ACPD
12, 5705–5738, 2012

Table 1. The $\Delta CH_3OH/\Delta CO$ ratio (in ppt ppb^{-1}) from the aircraft and TES from this study versus those from the literature.

$\Delta CH_3OH/\Delta CO$(ppt ppb^{-1})	Fuel/Location/Season	Source
41–44 (C-130) 26–39 (DC-8)	Urban outflow/Mexico City/March	This Study
18–24 (TES)	Urban outflow/Mexico City/March	This Study
42 ± 7 (TES)	Plants emissions/Amazon basin/August–September	This Study
21.0 ± 14.0	Urban plumes/California	Singh et al. (2010)
9.0	Urban plumes/New York City and Boston/summer	Warneke et al. (2007)
8.4	Urban plumes/Los Angeles/spring	Warneke et al. (2007)
4–11	Ground samples/Boulder and Pittsburgh/winter	Millet et al. (2005); Goldan et al. (2005)
14–28	Fire plumes/Mexico/spring	Yokelson et al. (2009)
19–32	Open fires/Mexico/spring	Yokelson et al. (2011)
9.6 ± 1.9	Fresh fire plumes/Canada	Simpson et al. (2011)
15.6 ± 9.2	Fresh fire plumes/Canada	Singh et al. (2011)
10.8 ± 4.4	Aged fire plumes/Alaska and western Canada	De Gouw et al. (2006)
14 ± 1	Forest fire plumes/Alaska	Goode et al. (2000)

ACPD
12, 5705–5738, 2012

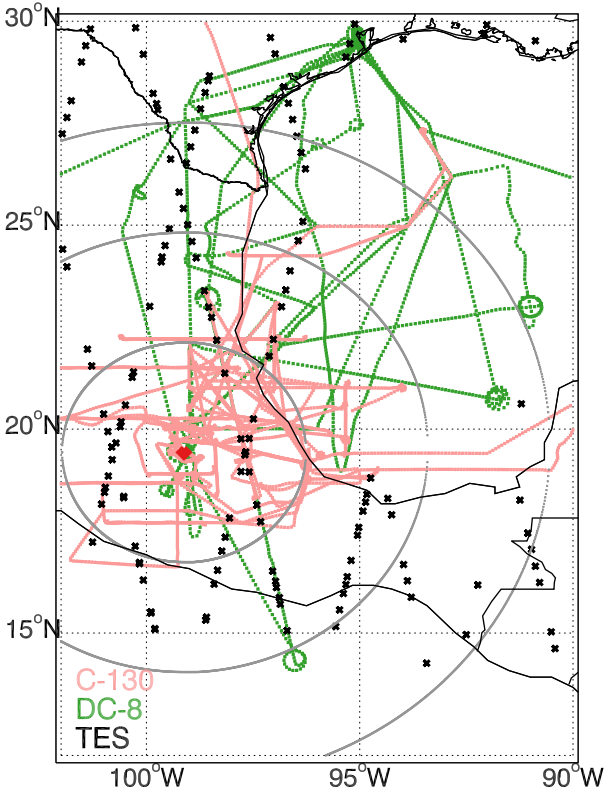

Fig. 1. Aircraft flight tracks (C-130 in pink, DC-8 in green) and TES footprints (black crosses) during MILAGRO. Circles show radii of 300, 600 and 900 km from the center of Mexico City (red diamond).

ACPD
12, 5705–5738, 2012

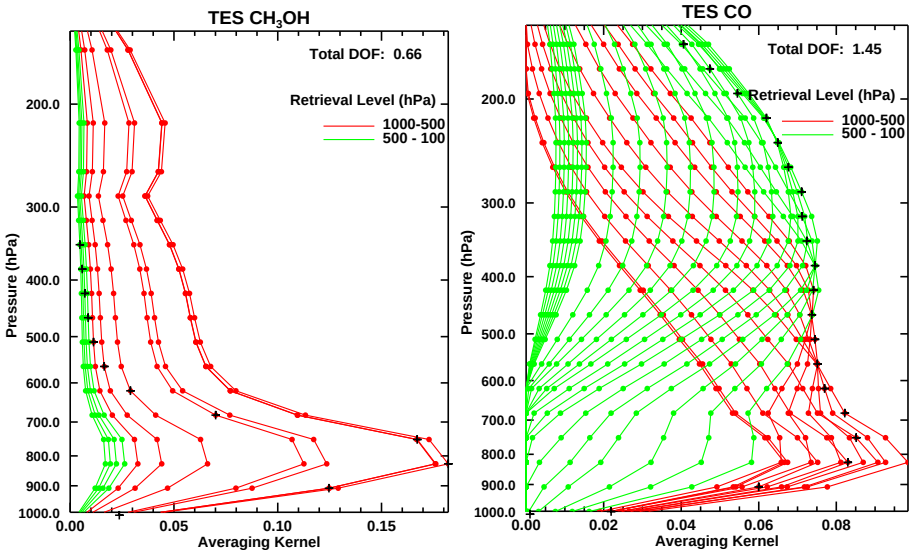

Fig. 2. Example TES averaging kernels for CH_3OH (left panel) and CO (right panel) from MILAGRO.

ACPD
12, 5705–5738, 2012

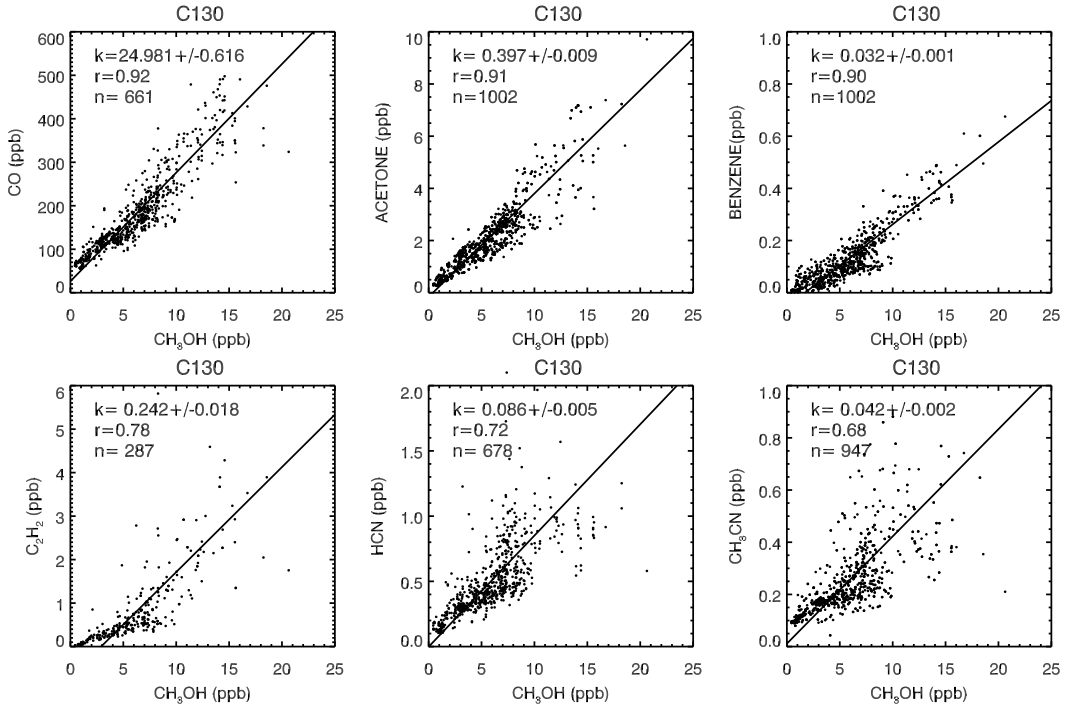

Fig. 3. Correlations between CH_3OH and a suite of gases (CO, acetone, benzene, C_2H_2, HCN and CH_3CN) from a subset of C-130 measurements near the source region (within 300 km of the Mexico City center and below 600 mb) during MILAGRO. Regression slopes (k), correlation coefficients (r) and the sample count (n) are shown.

ACPD
12, 5705–5738, 2012

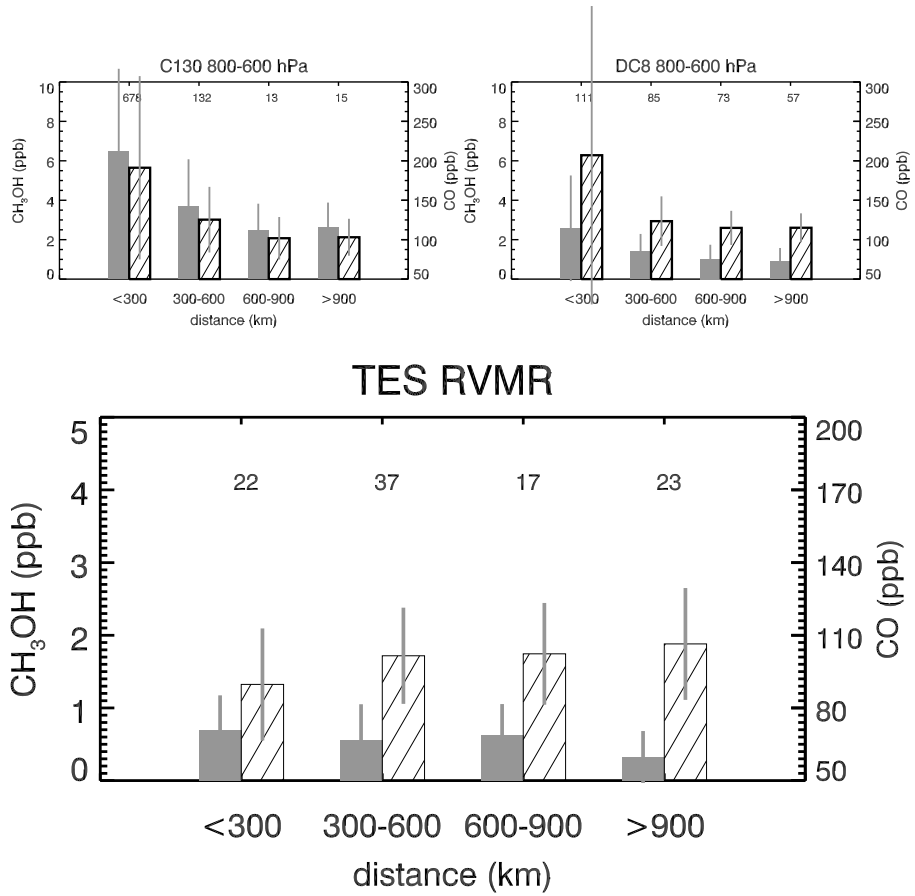

Fig. 4. Spatial variation of CH_3OH (grey bars, left axis) and CO (hatched bars, right axis) concentrations with distance from Mexico City Center during MILAGRO, based on the C-130 aircraft **(a)**, DC-8 aircraft **(b)**, and TES space-based **(c)** observations.

ACPD
12, 5705–5738, 2012

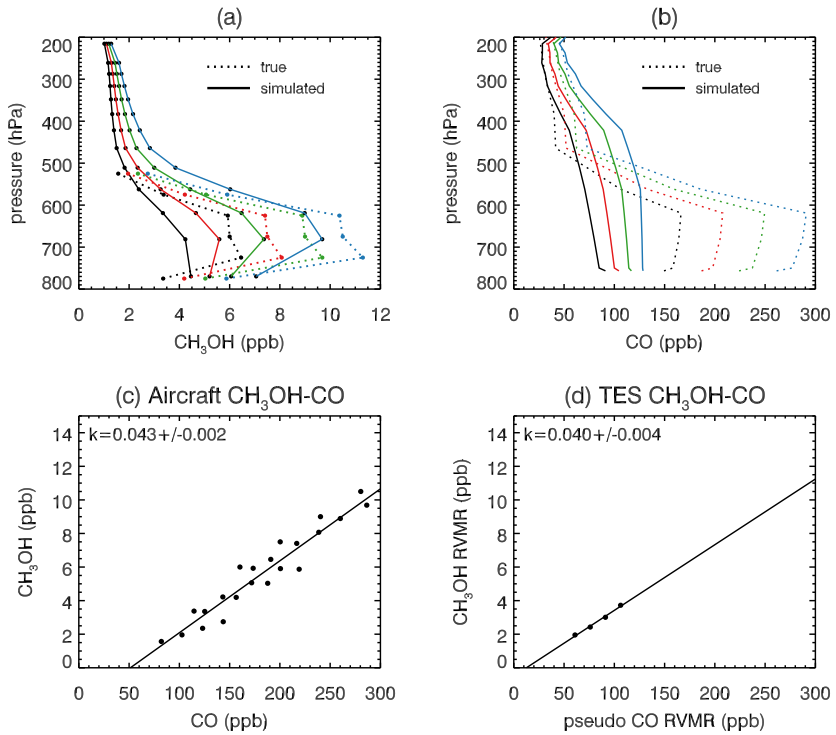

Fig. 5. Demonstration of the ability of TES to measure CH_3OH-CO enhancement ratios in the absence of systematic errors. **(a)** Dashed lines show representative CH_3OH profiles ("true" profiles) constructed from an ensemble of MILAGRO aircraft observations, and used to generate simulated TES radiances. The solid lines show results of the TES retrievals ("simulated" profiles) generated from simulated radiances with TES measurement noise added. **(b)** As Fig. 5a, but for CO. **(c)** The CH_3OH-CO correlation based on the actual input profiles (dashed lines in Fig. 5a and b). **(d)** TES derived CH_3OH-CO correlation based on the simulated retrievals (solid lines in Fig. 5a and b).

ACPD
12, 5705–5738, 2012

Methanol-CO correlations in Mexico City pollution outflow

Y. Xiao et al.

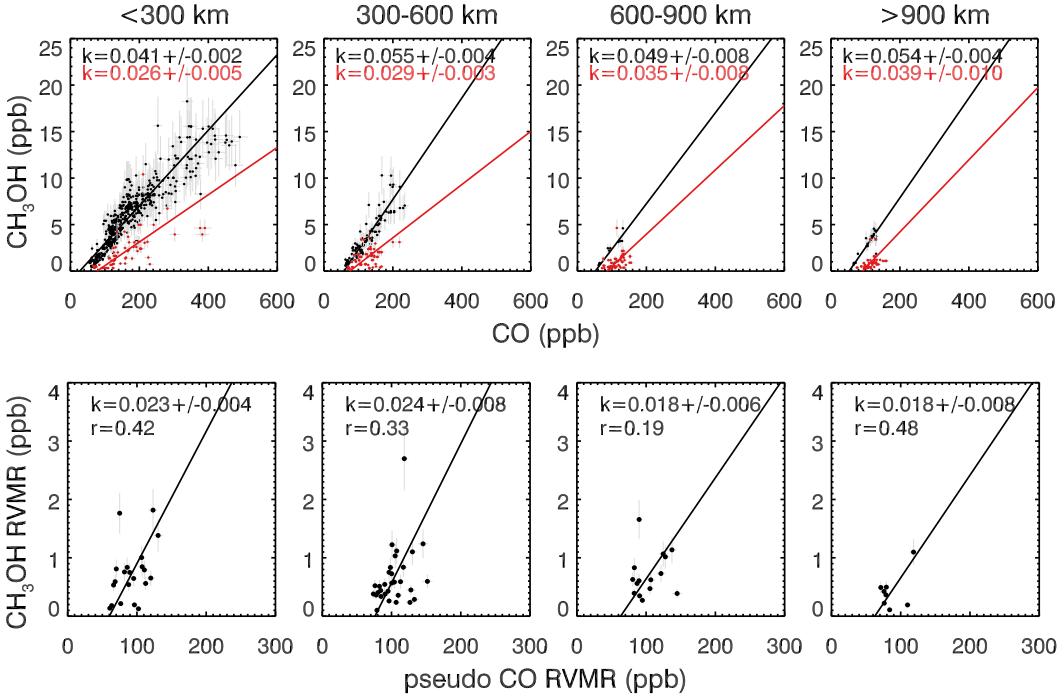

Fig. 6. CH_3OH-CO correlations in Mexico City outflow during MILAGRO, binned by distance from Mexico City Center. Upper panels show aircraft measurements (black for C-130 and red for DC-8). Lower panels show TES measurements.

ACPD
12, 5705–5738, 2012

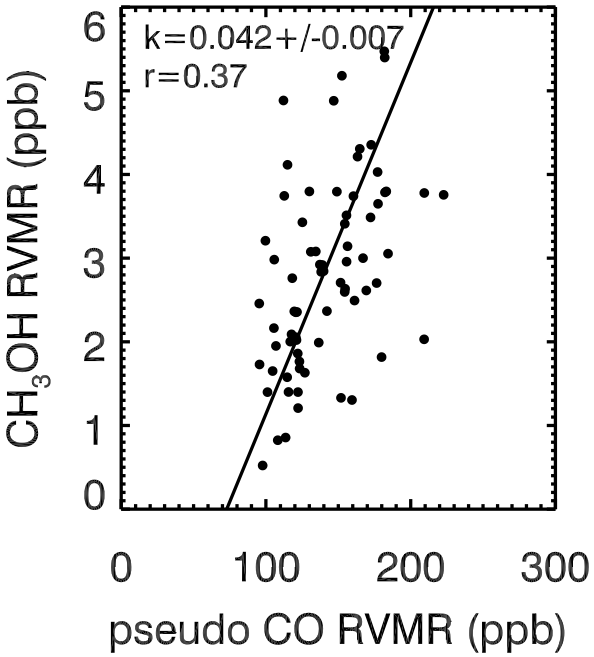

Fig. 7. CH_3OH-CO correlation derived from TES observations over the Amazon Basin (16.7° S–6.9° S, 63° W–49° W) during August–September of 2005.

ACPD
12, 5705–5738, 2012